Module 2 - Optical Fiber Materials

Dr. B.G. Potter

Professor, Material Science and Engineering Dept, University of Arizona

Dr. B.G.Potter is a Professor of Material Science and Engineering in the University of Arizona. Research activity within Dr. Potter's group is centered on the synthesis and study of glass, ceramic, and molecular hybrid materials for photonic and electronic applications. Active research and ongoing programs include: optically driven molecular assembly strategies, nanostructured photovoltaic energy conversion materials, photoactivated phenomena in glass and hybrid thin films, solution and physical vapor phase deposition of thin films and nanocomposites (oxides, inorganic-organic hybrids), thermal stability of complex oxide optical materials, environmental sensing, optical behavior of rare-earth-doped matrices, semiconductor quantum-dot ensembles, and optical spectroscopy.

Email: bgpotter@mse.arizona.edu

Introduction

Material selection and development for use in fiber-optic telecommunications is driven by a broad variety of, often conflicting, physical property and material processing considerations. Beyond the requirements imposed to meet passive and active optical performance needs (e.g. minimum propagation losses at the operational wavelength, mode propagation control, dispersion control, and optical gain bandwidth), the material must allow for the reliable and economic fabrication of desired fiber designs while providing sufficient performance stability under the environmental conditions anticipated for the application. This module will provide insight into the primary issues contributing to the selection of materials for fiber-optic telecommunications. The discussion will stress considerations addressing the intrinsic, or bulk, optical and physical properties important to the use of glassy materials (inorganic and organic (plastic)) in this context.

The properties of materials are intimately linked to the chemical elements present, their relative amounts (composition), and their bonding and interatomic arrangement to form the material structure. For optical fiber applications, we are interested in amorphous materials (glass). Such materials are those that exhibit a lack of long-range order or periodicity in their structure; in other words, materials in which there is no correspondence between the positioning of atoms across many interatomic spacings. Typically, however, these materials do exhibit a local order, forming consistent structural units of multiple atoms that are, themselves, randomly connected over longer distances to form an interconnected network. Of great interest to optical fibers, for

The authors would like to acknowledge support from the National Science Foundation through CIAN NSF ERC under grant #EEC-0812072.

example, is silica glass which exhibits structural units composed of a silicon atom connected to 4 adjacent oxygen atoms arranged at the corners of a regular tetrahedron. In contrast to quartz (a crystalline form of silica in which these structural units are interconnected in an ordered, repeating fashion), the silica tetrahedra in a glass are assembled randomly to form the three-dimensional network structure.

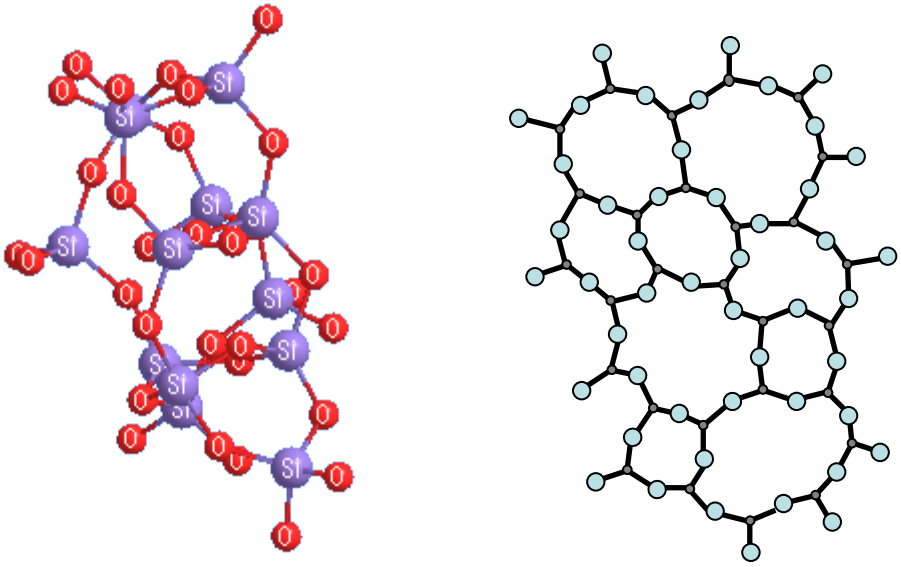

Figure 2.1: *Three and Two-dimensional illustration of silica tetrahedral network in a glassy structure. Note that the fourth oxygen atom in each tetrahedron will be connected to each silicon atom out of the plane of the drawing, thus forming the full three-dimensional network.*

It is the chemical identity and combination of local and long-range structural characteristics that dictate the physical properties exhibited by a given material. More to the point, by proper control of composition and structure through material formulation and processing, physical properties can be adjusted for a particular application. In the case of optical fiber materials, modifications in composition, for example, can be used to influence the refractive index of the glass. This enables the development of core and cladding compositions contributing to the overall fiber design and its light propagation characteristics. Similarly, appropriate thermal processing is often critical to ensure high quality glass rods (called preforms) that are used for fiberization. These glass rods must be free of small and large-scale structural and compositional inhomogeneities that can adversely affect optical transmission in the finished product by scattering.

The authors would like to acknowledge support from the National Science Foundation through CIAN NSF ERC under grant #EEC-0812072.

In general, then, key material optical and physical properties and behaviors of interest to the design and fabrication of fiber optic devices include:

1) Optical Properties:
   - Refractive index and index variation with optical wavelength (materials dispersion).
   - Optical loss (absorption, scattering, reflection) at the operational wavelengths of the fiber.
2) Thermal Properties
   - Thermo-rheological behavior, e.g. melting temperature, glass transition temperature (Tg), viscosity variation with temperature.
   - Material phase stability: crystallization temperature, tendency for phase separation (mixed amorphous phases of different composition).
   - Compositional stability under processing temperatures.
3) Mechanical Properties
   - Fracture strength and environmental sensitivity of fracture strength.
4) Chemical Properties
   - Sensitivity to the ambient environment stability.

These issues are linked through the glass compositions used and their corresponding atomic structure. Thus, materials selection often requires compromise to obtain targeted bulk optical behavior (e.g. refractive index, minimal optical loss at operating wavelength) while simultaneously providing materials that allow the thermal processing (preform development, fiber drawing) necessary to achieve the required fiber device design (core-clad geometry, index profiles etc.).

We will see that material thermal and chemical characteristics determine the preform development and fiberization methods available for use with different inorganic glass systems. The treatment of this subject will focus on the silica-based fiber materials that form the basis for the majority of fiber systems for telecommunications.

Fiber fabrication methods can be classified into two basic approaches:

1) Preform methods
2) Double crucible methods.

The vast majority of telecommunications and specialty glass optical fibers are produced via preform methods, involving the initial production of a macroscopic glass rod that embodies the targeted core-to-clad diameter ratio and refractive index profile needed in the final optical fiber. Compared with the optical fiber diameter (typically 125 microns), the preform is much larger

The authors would like to acknowledge support from the National Science Foundation through CIAN NSF ERC under grant #EEC-0812072.

with outer diameters in the 10-25 mm range and lengths up to 120 cm long. Localized re-heating of the preform above the glass transition temperature allows it to be elongated (drawn) into fiber form while retaining the preform's original core-clad glass radius ratio.

Some, typically low temperature melting glass systems (e.g. chalcogenides) allow the production of fibers of these glasses directly from the melt using specialized crucible designs to allow the simultaneous melting and drawing of the core and clad compositions (double crucible). Both perform-based and direct melting based fiber drawing processes will be addressed later in the module after a discussion of fiber geometry.

2.1 Optical Properties

At a fundamental level, the bulk glass used for an optical fiber dictates the primary characteristics of its interaction with light. These characteristics, in turn, serve as the basis for subsequent device design and the overall performance of the fiber. The present discussion will provide a brief overview of contributions to optical properties intrinsic to the material. The student is referred to subsequent modules dealing with wave propagation in heterogeneous media and propagation related issues in fibers (Modules 3 and 4) for additional insight into the ramifications of intrinsic material properties on fiber behavior and its optimization.

The Optical Constants

The propagation characteristics of light within a medium (in this case, a glass) are dictated by the complex refractive index:

$$n(\omega) = n'(\omega) + in''(\omega) \qquad \textit{(Equation 2.1)}$$

where n'' is called the extinction coefficient and n' the real index of refraction of the material; together these are often referred to as the optical constants of the material. These terms dictate both how fast the light travels through the material, or its phase velocity, and how quickly the light intensity is lost with distance traveled in the medium, respectively. The complex refractive index is, itself, directly related to the high-frequency complex dielectric function,

$$\epsilon_D(\omega) = n(\omega)^2 = \epsilon_1(\omega) + i\epsilon_2(\omega)$$

that dictates the nature of interaction between the material and electric and magnetic fields.

The authors would like to acknowledge support from the National Science Foundation through CIAN NSF ERC under grant #EEC-0812072.

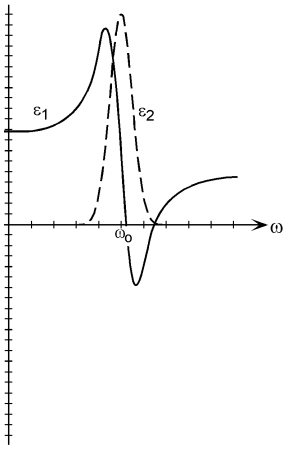

Figure 2.2: *The real and imaginary parts of the complex dielectric function with frequency.*

It is extremely important to note that both of these *optical constants* in fact, vary with optical frequency ω. The index of refraction and extinction coefficient are said, therefore, to exhibit a frequency or wavelength "dispersion". The general nature of the dispersion can be obtained through relatively straightforward treatment of a damped simple harmonic oscillator driven by an oscillating field. The figure above shows the behavior of the real and imaginary components of the complex refractive index based on a collection of oscillators with a single characteristic or resonance angular frequency, ω_o.

It can be seen in the Figure that the extinction coefficient, κ, exhibits a peak at ω_o. This is accompanied by a characteristic behavior in the refractive index, n, in which the dependence of n on ω can be observed. It can be shown that the reflectivity for the oscillator ensemble is a function of both n and κ, and also exhibits a distinct band of maximum reflectivity associated with the ω_o resonance region. The more complicated behavior of real materials arises from the motion of constituent bound electrons (electronic transitions) and atomic nuclei (vibrational transitions) in response to the applied optical field. As we will see, the optical behavior of materials for optical fiber applications can be modified through changes in composition and structure.

If we write an expression for the time and space dependent amplitude of a plane wave in a material (1-D),

$$E(x,t) = E_0 e^{\frac{-\omega n'' x}{c}} e^{i\omega\left(t-\frac{n'x}{c}\right)} \qquad \textit{(Equation 2.2)}$$

The authors would like to acknowledge support from the National Science Foundation through CIAN NSF ERC under grant #EEC-0812072.

where c is the speed of light. Notice that both the space and time dependence of the wave amplitude depends upon both components of the complex refractive index.

Fiber Performance Metrics

Fundamental optical phenomena of direct impact to the behavior of fiber optic devices (e.g. transmission behavior, mode propagation, group velocity etc.) originate from the optical constants of the materials involved.

One of the most direct correlations between a material optical constant and an important fiber performance metric is found in the extinction coefficient. Referring again to the equation for the complex refractive index, it can be seen that the amplitude of a propagating wave decreases in an exponential fashion with propagation distance at a rate dictated by the extinction coefficient. Recognizing that the light intensity of an optical wave is given by I = EE* (where E* is the complex conjugate of the electric field expression) we find that the intensity of light is decreased exponentially as light travels through the material according to:

$$I = EE^* = I_o \exp\left(-\frac{2\omega n'' x}{c}\right)$$
$$where: I_o = E_o^2$$

(Equation 2.3)

We can re-write Equation 3 in terms of the material absorption coefficient, α:

$$I_t = I_o \exp(-\alpha x)$$
$$where: \alpha(\omega) = \frac{2\omega n''}{c}$$

(Equation 2.4)

where I_t is the intensity of light transmitted through the material. The expression for I_t is known at Beer's Law. Examination of the above equations, shows us that the intensity of light propagating through an attenuating (absorbing or "lossy") medium will exhibit an exponential decay with increasing distance of propagation.

The authors would like to acknowledge support from the National Science Foundation through CIAN NSF ERC under grant #EEC-0812072.

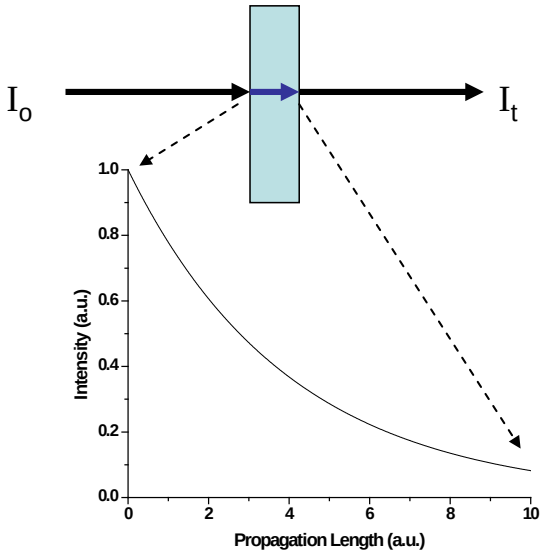

Figure 2.3: *Exponential decay of transmitted intensity in an absorbing material.*

Again, α will also vary with frequency (wavelength) as does the extinction coefficient. Direct measurement of the material absorption coefficient is often readily available through spectroscopic measurement of material transmission.

Clearly, fiber optic operational wavelength bands in which α is small are desired for the development of fibers intended for use over long transmission distances with low optical signal loss. Hence, the selection of glass compositions is often dictated by the anticipated operational wavelength ranges targeted by the application. We will revisit this issue later in the module when specific glass systems used in fiber optic applications are discussed.

Similarly, the real portion of the refractive index (and its dispersion) within the optical fiber dictates the propagation characteristics of different wavelengths within the fiber and the interaction of light with interfaces between materials (e.g. reflectivity, scattering). Wavelength dependent propagation characteristics in telecommunication fibers, for example, can place fundamental limits on data transmission rates since data transmission makes use of short optical pulses that are composed of a broad spectral band (transform-limited or compressed pulses). The refractive indices (and the associated index differences between them) in an optical fiber, also determine such important fiber properties as numerical aperture and V-number. These properties will be taken up in subsequent modules.

For real materials, the dispersive behavior of κ is most often found through measurement of the material absorption spectrum. While direct measurement of refractive index is also pursued, the index dispersion for a variety of technologically significant glasses in frequency ranges below the primary electronic absorption resonance can be calculated using the Sellmeier relationship

The authors would like to acknowledge support from the National Science Foundation through CIAN NSF ERC under grant #EEC-0812072.

$$n^2(\lambda) - 1 = \sum_{i=1}^{n} \frac{A_i \lambda^2}{\lambda^2 - \lambda_i^2}$$

(Equation 2.5)

Sellmeier coefficients (A_i) have been measured for many materials, particularly those glasses used for optical fibers.

Using these empirically determined parameters, the refractive index can be computed at any wavelength of interest within the limits of applicability of the parameters. The index dispersion for a number of oxide glasses can be found in a number of references (e.g. Optical Materials, Simmons and Potter, Academic Press, 2000) and is given below for silica glass and for a common optical fiber composition of silica glass doped with 5 mol% germanium dioxide (GeO_2)as an example.

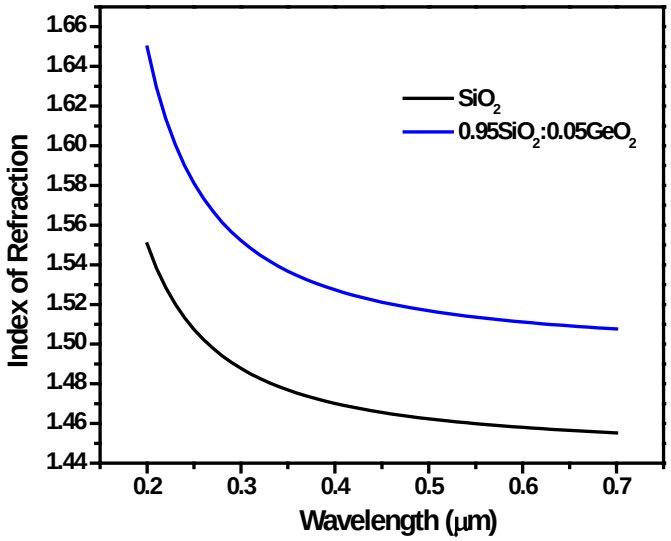

Figure 2.4: *Refractive index dispersion for silica glass and for germanosilicate glass over the visible portion of the optical spectrum.*

Refractive index and extinction coefficient also contribute to phenomena associated with interfacial reflection and scattering. The Fresnel equations for light incident at an interface provide a means to determine the reflected and transmitted light amplitude at a material discontinuity (e.g. glass-air, core glass-cladding glass) in terms of both the index and extinction coefficient. For normal incidence light at an interface, these equations simplify to expressions for the reflection and transmission intensity coefficients (known as reflectance, R, and transmittance, T).

The authors would like to acknowledge support from the National Science Foundation through CIAN NSF ERC under grant #EEC-0812072.

$$R = \frac{(n_i - n_t)^2 + n''^2}{(n_i + n_t)^2 + n''^2} \quad and \quad T = \frac{4n_i^2}{(n_i + n_t)^2 + n''^2}\left(\frac{n_t}{n_i}\right) \qquad \textit{(Equation 2.6)}$$

where R and T are the reflection and transmission intensity coefficients; $n_{i,t}$ is the refractive index of the incident and transmission medium, respectively.

In a region of low absorption, i.e. at the operational wavelength for a high transmission fiber, and at normal incidence, the reflection is determined by the refractive indices involved. In the context of fiber optics, this would provide information of interest for reflection losses at interconnections and its wavelength dependence (through the index dispersion).

2.2 Thermal Properties

While bulk optical behavior is the primary metric in the selection of a glass for optical fiber applications, other material properties and associated fiber fabrication concerns often mitigate the successful synthesis and application of these glasses in a fiber context. The compositional variation that provides the necessary refractive index step between the fiber core and cladding, for example, may also produce a variation in the viscosity between the two glasses at the fiber drawing temperature that makes the practical production of the required fiber geometry difficult or intractable.

The coupling of optical properties with other physical phenomena through glass composition and structure and the challenges associated with the simultaneous thermal processing of multiple glass compositions, inherent in the production of optical fibers, motivates compromise in material selection and has also resulted in engineering developments in fiber fabrication tools, approaches, and methodology. With the previous discussion of optical properties in hand, we will now provide a brief background for some of the non-optical phenomena and properties that are often critical to the evaluation and use of materials for optical fiber applications. The following discussion will deal with general material phenomena or those specific to silica (SiO_2)-based fibers. Issues specific to other glass systems will be included, as needed, in a later section.

While the optical constants (and the associated optical phenomena) described above do exhibit some dependence on material temperature, the thermally dependent characteristics of a glass in the present discussion will address those properties that impact the successful elevated temperature processing of the material (i.e. preform synthesis and fiberization). This information will provide a basis for the fabrication technology discussion in Module 2.

Glass Viscosity

Optical fibers are thin cylindrical structures comprised of an inner “core” region surrounded by an outer “clad” region. In order for light to propagate inside the core region of the fiber, it is necessary that the core and clad regions have different refractive indices (in particular $n_{core} > n_{clad}$ must be true). In the context of optical fiber fabrication,then, dissimilar glasses (for the core and

The authors would like to acknowledge support from the National Science Foundation through CIAN NSF ERC under grant #EEC-0812072.

clad regions of the fiber waveguide) are formed into a preform defining the required core-clad geometry that is subsequently reheated to allow fiber drawing. This process is intimately linked to a reduction in resistance of the glass to permanent deformation under an applied shear stress at the draw temperature. To first order, the rate at which the glass deforms (strain rate) can be related to the applied shear stress through the linear viscosity:

$$\tau = \eta \dot{\varepsilon} \qquad \textit{(Equation 2.7)}$$

Where $\dot{\varepsilon}$ is the strain rate, τ is the applied shear stress, and η is the viscosity. The viscosity of glass typically varies by many orders of magnitude over temperatures ranging from room temperature to those in excess of 1400 °C for common silicate-based glasses. The mechanical behavior of the glass can, thus, be broadly varied, from brittle solid to low-viscosity liquid, through temperature control. The viscosity behavior is associated with thermodynamic and structural kinetic factors fundamental to the glassy state that are related through the glass structure itself.

Clearly, the variation of glass viscosity with temperature will be important in determining such processing conditions as the temperature necessary for fiber drawing and the drawing speed (strain rate). A large variation in viscosity will narrow the processing temperature range acceptable for drawing to avoid problems such as breakage (low viscosity) or insufficient diameter uniformity. Similar viscosity vs. temperature profiles between core and cladding glass compositions are also required to ensure high-fidelity reproduction of the preform refractive index profile. It is also important to recognize that the relationship provided in the viscosity equation assumes a linear, or Newtonian, viscosity behavior between the shear stress and strain rate. In many cases, glasses can exhibit nonlinear viscosity behavior, showing for example, increasing (shear thickening) or decreasing (shear thinning) viscosity with changes in strain rate. Such properties, again, can impact the fiberization conditions (e.g. draw speed, temperature) used.

Glass Forming Ability and Stability

In addition to the need for close control of glass viscosity for drawing, it is important that the homogeneity and anticipated optical and physical behavior of the glasses involved be retained after the fiber is formed.

Thus, it is important to note that the single-phase amorphous structure of the glass does not represent the lowest thermodynamically stable energy state and that lower energy structures exist, characterized by the presence of multiple material phases, either crystalline or amorphous in nature. The formation of these phases is avoided during initial glass melting by rapid cooling (quenching) of the liquid melt into the glass transformation range. The minimum rate necessary to cool a glass melt without crystallization is called the critical cooling rate (CCR). The elevated temperatures used to enable fiber drawing, however, bring the glassy material back

The authors would like to acknowledge support from the National Science Foundation through CIAN NSF ERC under grant #EEC-0812072.

above the glass transition range, thus activating the atomic and larger scale molecular rearrangement (reduced viscosity) that will enable the development of lower energy material structures (i.e. crystallization).

The stability of a glass, i.e. its resistance to such structural transformation processes as crystallization or phase separation, is another thermal property of importance to the successful production of fiber optics. If crystallization or the formation of a second amorphous material phase (phase separation) occurs at the draw temperature, for example, the glass drawing properties (e.g. viscosity) can be altered, impacting the draw conditions with time. Of perhaps even greater concern is the property degradation associated with these embedded phases that often possess different optical and physical properties than that of the parent glass. These phases can contribute to the formation of inhomogeneities in the final glass fiber that can produce enhanced optical scattering, optical loss/attenuation, and degradation of mechanical and chemical properties.

In terms of crystallization (also referred to as devitrification), glass stability is often described in terms of readily obtained calorimetrically determined temperatures that are associated with key thermodynamic and kinetic processes contributing to phase transformation. One criteria used to evaluate glass stability, for example, corresponds to the difference in temperature between the glass transition, T_g, (where increased structural mobility becomes activated) and the thermodynamic crystallization point, T_x, for the corresponding crystal.

$$\Delta T = T_x - T_g \qquad \textit{(Equation 2.8)}$$

These temperatures can be determined by an analysis of differential scanning calorimetry (DSC) data obtained from a representative glass sample. The larger the temperature difference observed, the less rapid crystallization is anticipated to proceed when the glass is heated beyond the glass transformation range (and, conversely, the lower the critical cooling rate necessary for glass formation).

Compositional changes in the glass can significantly impact stability through modification of the crystallization or phase separation temperatures. This directly impacts the suitability of the glass for fiber production as the core-clad refractive index contrast needed is often obtained through compositional variation. A broad glass formation and stability range is needed to allow the optical performance of the fiber to be tailored without significant impact to fiber manufacturability. Thus, both thermodynamic and kinetic factors, mediated by the chemistry and thermal history of the glass, will contribute to its stability and suitability for fiberization.

It is also important to note that, beyond the thermodynamically driven formation of discrete separate phases upon heating, the characteristics (and associated properties, e.g. density, refractive index) of the glass structure itself are a product of the glass thermal history of formation. Thermal excursions beyond the glass transition range associated with preform

The authors would like to acknowledge support from the National Science Foundation through CIAN NSF ERC under grant #EEC-0812072.

formation and/or fiberization can therefore result in the modification of these properties. Additional information regarding the nature of the glassy state and its formation are provided in the graduate module on Advanced Materials Issues.

2.3 Mechanical Properties

Mechanical properties, including hardness and failure strength, dictate the viability for fiber application under anticipated handling and use conditions. Like crystalline ceramics, the inorganic glasses used in telecommunications fiber optic fabrication are brittle, exhibiting failure through crack formation and propagation without significant permanent (plastic) deformation of the material under the stresses producing the failure.

Applied stress and Crack Propagation

In contrast to ductile materials, failure processes in brittle solids are typically associated with the presence of localized structural flaws within the material volume or at surfaces or interfaces in the structure. These flaws can be of varying sizes, size distributions and types, arising from such issues as scratching during processing/handling, foreign particles at surfaces, or variation in fiber geometry due to changes in draw conditions during fiber production.

Under tensile stress conditions, flaws can serve to concentrate the applied stress producing local stress levels sufficient to further disrupt the glass structure and allow crack growth (propagation). It is the presence of flaws and the associated stress concentration that results in observed failure strengths in glass and ceramics that are often 5 – 20X lower than that anticipated from theoretical intrinsic strengths based on the cohesive bond strength of the constituent atoms.

Using formalism developed by Griffiths [*Phil. Trans. Roy. Soc.* A221:163, 1920], the critical applied stress sufficient to enable crack propagation from an elliptically shaped flaw can be evaluated in terms of a balance between the energy increase associated with the formation of new surface area (proportional to the solid-vapor interfacial energy, Γ_{sv}) and the release of local elastic strain energy as the crack lengthens in a brittle solid (Griffith criterion).

The stress intensity factor, K, combines the contributions of both applied stress and flaw geometry to provide a means to evaluate the potential for crack propagation. K is given as

$$K_I = Y\sigma\sqrt{\pi c} \qquad \textit{(Equation 2.9)}$$

where the stress field and geometry of the crack tip are defined according to **Figure 2.5**, which gives the example of an elliptical flaw. In the equation, Y is a dimensionless parameter, dependent upon the crack and specimen sizes and geometries. Note that as the length of the crack, c, or the applied tensile stress, σ, increases, the value of Y, and the overall intensity factor increases. The subscript, I, of the stress intensity factor corresponds to a specific crack propagation mode denoting the relationship between the applied stress field and the crack surface displacement.

The authors would like to acknowledge support from the National Science Foundation through CIAN NSF ERC under grant #EEC-0812072.

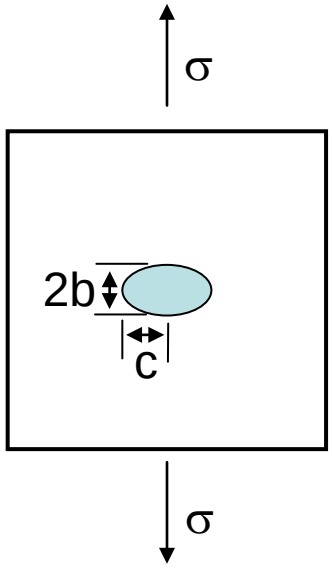

Figure 2.5: *Elliptical flaw in a glass plate that is placed under tension.*

It is clear, therefore, that the strength of a glass is dependent both on the stress applied and on the geometry of flaws in the glass. A number of crack extension modes are shown in **Figure 2.6**.

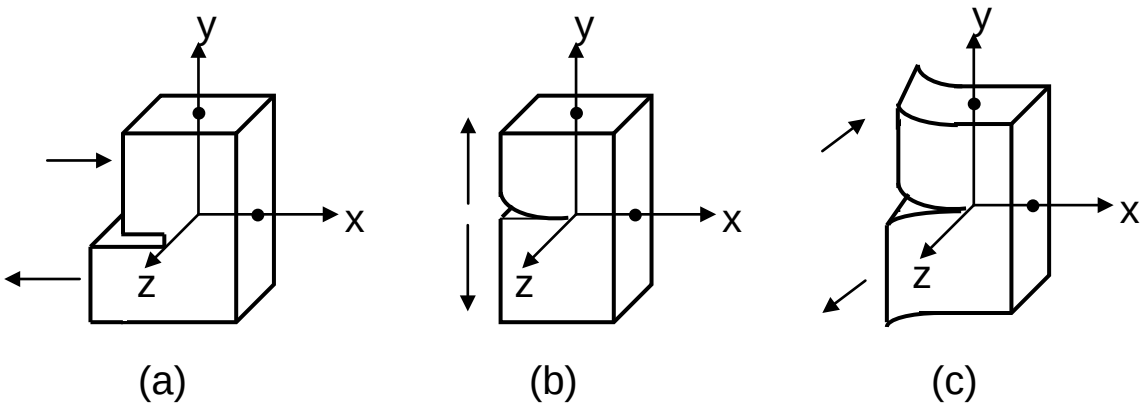

Figure 2.6: *Different modes of crack propagation (a) sliding, (b) opening, and (c) tearing.*

The critical stress intensity factor, K_{Ic}, corresponds to the K_I value at which crack propagation and brittle failure occur. Often called the "fracture toughness." it is used as a metric to compare material resistance to catastrophic crack growth under an applied stress. For example, with the K_{Ic} value, flaw size, and Y parameter known, the failure stress may be determined. Clearly, the size and geometry of the flaw will directly impact the development of local stress, with larger flaw sizes reducing the applied stress necessary to produce failure (i.e. the failure stress).

The authors would like to acknowledge support from the National Science Foundation through CIAN NSF ERC under grant #EEC-0812072.

In a fiber possessing a range of flaw sizes, shapes and locations, the larger flaws will generally serve as the weakest points in the fiber, causing catastrophic failure at lower stresses. This "weakest link" picture for fracture strength in glass leads to a distribution of observed fracture strengths that reflects the underlying flaw distribution present in the as-received fiber. If the flaws are assumed to be independent and randomly distributed and if fracture is assumed to occur at the largest flaw, the brittle fracture strength for a population of glass specimens can be described in terms of a Weibull-type distribution, leading to an expression for the total cumulative probability that a fiber of length L will fail below a given stress level, sigma.

$$F(\sigma, L) = 1 - \exp\left[-\left(\frac{\sigma}{\sigma_o}\right)^m \frac{L}{L_o}\right] \qquad \textit{(Equation 2.10)}$$

where: m = the Weibull modulus (measure of the width of the strength distribution) and σ_o and L_o refer to a characteristic stress and specimen length, respectively for the fracture strength distribution. Note that the sampled volume (or in this case, the length) of the specimen directly impacts the probability for failure. For longer samples, the probability that sufficient stress for failure will be applied at a larger flaw increases and more consistent sampling of the overall flaw size distribution is anticipated.

For a population of brittle material specimens satisfying a Weibull distribution, the length term in the above expression is often removed and a plot of ln(ln(1-F)) vs. ln(σ) (the Weibull plot) will exhibit a straight line whose slope given by the Weibull modulus,m. Such plots are useful in the evaluation of fracture strength variability between materials and sample processing conditions. A larger Weibull modulus, for example, indicates a narrower distribution of failure stresses.

Mechanical and Environmental Factors Contributing to Strength

The precise nature of the applied stress field and the environmental conditions at the crack tip will also dramatically impact the characteristics of crack formation, propagation and failure behavior obtained. Of primary interest is the fact that the above description for brittle fracture does not include the time dependence of the processes involved. The coupled effects of time dependent applied stresses or strains (often experienced in application environments) and chemical and structural processes occurring at the crack tip can lead to higher fracture probability at lower applied stress than that anticipated from the constant strain rate, controlled environment studies often used to evaluate fiber strength characteristics. The development of fiber qualification tests that accurately reflect actual service conditions with regard to stress/strain and environment (e.g. relative humidity) is therefore critical for valid evaluation of fiber mechanical behavior.

As an example, an investigation of the effect of local environment on the tensile strength of silica fibers shows that under conditions leading to a reduction in moisture at the glass surface, i.e. low

The authors would like to acknowledge support from the National Science Foundation through CIAN NSF ERC under grant #EEC-0812072.

temperature or vacuum conditions, the failure strengths observed for the glass are high and essentially time independent. However, under conditions leading the presence of environmental moisture, delayed failure under a constant stress, often referred to as "static fatigue", is observed. In silica-based fibers, fatigue has been associated with the combined effect of stress and water attack (hydrolysis) at the crack tip, i.e. "stress corrosion", leading to enhanced crack propagation velocities under stress. In this case, hydrolysis at strained siloxane bonds is a primary mechanism:

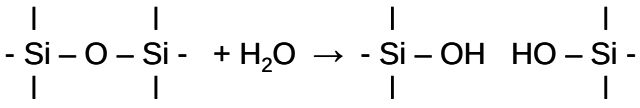

-Si – O – Si - + H2O == - Si –OH HO – Si - *(Equation 2.11)*

In a related behavior, silica fiber stored under zero stress conditions can also show degradation in strength with time, referred to as "aging". The effect on strength can be observed both in terms of tensile strength and fatigue behavior and has been attributed to localized variation in water attack on the silica surface leading to roughening (increases flaw severity). Silica (and silica-based) glasses are known to exhibit fluctuations in structure and composition, giving rise to local changes in susceptibility to water attack and dissolution [Kurkjian in Mendez, and Innis, 1993].

Given the sensitivity of fiber mechanical behavior to surface mechanics and chemistry, fiber optics are coated with polymeric and/or metallic materials primarily as a means to minimize handling-induced surface flaws. While these materials typically are effective in isolation of the glass surface from liquid-phase water, true hermetic coatings, restricting permeation to water vapor and environmental gases, are utilized more infrequently. Additional discussion of fiber coating materials will be pursued in the next Module.

2.4 Chemical Properties

The relationship between the electronic and vibrational properties of the material, the associated optical behavior, and the material structure provide a fundamental means to characterize, evaluate, and select materials for use in optical fibers for targeted transmission and wave propagation performance. Indeed, beyond the selection of different glass compositions and glass forming systems, the use of ionic or molecular impurities can also be used to modify the electronic and vibrational states, and associated optical transitions, allowing the magnitude of the optical constants and their frequency dispersion to be altered or to provide new functionality (e.g. fiber-based optical amplification/lasing)

The precise nature of the magnitude and dispersion in the optical constants characterizing the glass arises from the composition (including impurities) and structure of the glass involved. Expanding from our earlier use of a hypothetical single-oscillator material, significant insight into the origin of dispersion (frequency dependence) in real materials can be obtained if the material is viewed as a collection of oscillating structural elements with varied resonance frequencies and this collection of oscillators is driven by an oscillating field (i.e. light). In this

The authors would like to acknowledge support from the National Science Foundation through CIAN NSF ERC under grant #EEC-0812072.

case, the overall magnitude and dispersion behavior of the optical constants is obtained as the sum of contributions from all oscillators participating in the interaction with the incident light. This is, of course, dependent upon the resonance characteristics of the oscillators involved, which is ultimately linked to the structural nature of these oscillating units. Clearly, contributions to the magnitude of the refractive index and extinction coefficient at a given operational frequency may arise from oscillators with resonance frequencies detuned from that operational frequency given the characteristic frequency dependence of both n and κ about a resonance (see earlier discussion).

Specifically, we can view the allowed motions of electrons and atomic nuclei (vibrations) within the material structure in this context. Higher frequency (shorter wavelength) material responses are typically associated with optical transitions involving bound electrons and their allowed energy states, contributing to the refractive index and extinction coefficient behavior in the visible and ultraviolet wavelength ranges while vibrational transitions involve lower frequency behavior associated with the motion of atomic nuclei about their equilibrium positions in the structure, contributing to optical constant dispersion in the long-wavelength visible and infrared.

Inorganic Glass Systems

As an example of the sensitivity of optical properties to variation in glass composition, **Figure 2.7** depicts the refractive index of silica glass as a function of common dopant concentration. The refractive index can be both increased and decreased by dopant addition. This is, in fact, a key method for the production of the necessary core-clad refractive index contrast necessary to sustain guided wave modes within the fiber structure. Common core-cladding combinations based on silica glass include: GeO_2-SiO_2 core, SiO_2 cladding; P_2O_5-SiO_2 core, SiO_2 cladding; SiO_2 core, B_2O_3-SiO_2. In addition to cationic (metal atom) substitutions, fluorination (F substitution for oxygen in the structure) can also be used to reduce the index of cladding glass.

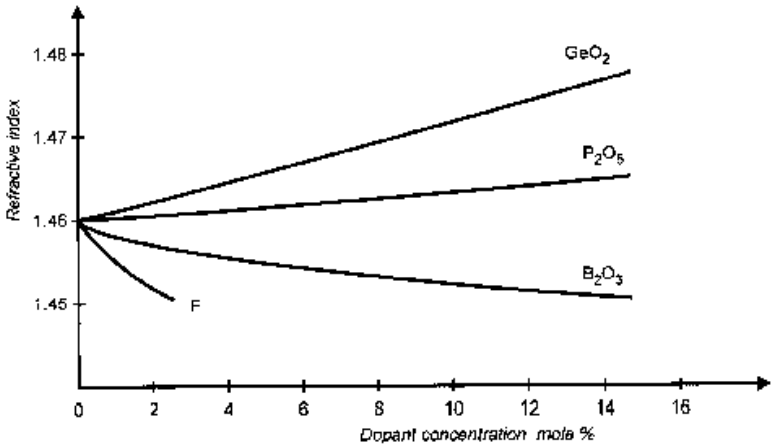

The authors would like to acknowledge support from the National Science Foundation through CIAN NSF ERC under grant #EEC-0812072.

Figure 2.7: *Dependence of the visible refractive index of doped silicate glasses on composition.*

As mentioned earlier, other material physical properties and phenomena are also coupled to optical behavior through glass structure and composition. Thus, while optical properties may be a primary factor in selecting materials for a particular fiber application (e.g. to provide specific operational transmission bands), it is often a full analysis of the associated mechanical, thermal, and chemical properties of a candidate glass that will provide the most appropriate selection. The table below summarizes some key thermal, optical, and mechanical properties of oxide (in this case, silica) and non-oxide glass systems used in the production of fiber optics and highlights the need for compromise in properties. In should be noted also that, like the silica glasses depicted in **Figure 2.7** above, one other important criteria for glass systems for fiberization includes the need for a broad glass forming compositional range to allow variation in composition for refractive index modification without significant changes in thermal properties (viscosity behavior, glass stability).

Table I

Selected Properties of Fiber Optic Glass Systems

[Values from "Infrared Fibers and Their Applications", J.A. Harrington; C.R. Kurkjian and M.J. Matthewson in "Specialty Optical Fibers Handbook", A. Mendez and T.F. Morse, Ed.; Handbook of Optics, Vol II, M. Bass, Ed.]

	Glass System			
Property	**Silica**	**Borosilicate (R_2O-JO-B_2O_3, SiO_2 (where R1 = alkali metal, J = alkaline earth)**	**Chalcogenides**	Heavy Metal Fluorides (HMF)
T_g (C)	1150	600-900	200-300	**250-400**
Thermal Expansion coefficient (10^{-6} /K)	5	7-12	10-60	**15-20**
Young's Modulus (GPa)	72	60-80	10-20	**50-65**
Density (g/cm^3)	2.20	2.5 – 3.5	3-5	**4-6**
Refractive	1.458 (587.6)	1.5-1.6 (587.6)	2.3 – 2.8 (1000)	**1.5 – 1.58 (589.6)**

The authors would like to acknowledge support from the National Science Foundation through CIAN NSF ERC under grant #EEC-0812072.

index (at λ, nm)				
Optical transmission range (nm)	**160-3800**	**300-2700**	**650-15000**	**250-7700**

Inorganic glasses used in fiber optics can be grouped into three main compositional systems, defined in terms of the primary anionic constituent: oxides, halides, and chalcogenides. The increasing mass of the anion, moving from oxygen (oxide) to fluorine, chlorine, bromine (halide) to sulfur, selenium, tellurium (chalcogenide), produces a corresponding reduction in vibrational energy for the glass, increasing its transparency in the infra-red region of the spectrum and reducing the probability for vibrationally mediated, non-radiative relaxation processes in emissive dopants. While significant variations in optical behavior can be attained through compositional variation (mixed metal, mixed anion stoichiometry), some generalizations regarding the property characteristics for each system are possible.

In terms of absorption behavior inorganic glass compositions are available with a broad range of transmission bands (i.e. the frequencies or wavelengths over which optical losses are very low). It can be observed that the material transmission band generally extends further into the near and mid-IR wavelength ranges as the atomic weights of the atoms involved in the glass structure increase, leading to lower frequency vibrational resonances and a delay in optical energy absorption (i.e. reduced %T) to longer wavelengths. This long wavelength transmission, while of limited interest for long-haul telecommunications operating in the 1.54 micron wavelength band, is of great interest for remote environmental sensing, spectroscopic analysis, biological monitoring, and optical delivery applications in the deeper infrared.

Some specific comments concerning inorganic glass forming systems are provided below:

***Oxides*:** In terms of fiber optic telecommunications, silica glass is the most commonly used glass system. Silica glass (SiO_2) and silicate glass systems (based on SiO_2 as a primary constituent) provide high stability to devitrification and offer broad glass forming compositional ranges allowing ready variation in refractive index. These glasses also typically exhibit some of the lowest absorption coefficients within the operational wavelength bands that are useful for telecommunications (most notably, 1.54 microns). The chemistry of silica and its precursors also aides in the production of high purity fiber preforms via vapor phase, chemical vapor deposition methods (see Module 2). Given the widespread use of silica-based systems, these are also typically the most highly studied fibers in terms of their mechanical behavior, chemical and thermal response.

In addition to compositional modification of silica through addition of other glass forming materials (e.g. B_2O_3, GeO_2) and modifiers (e.g. alkali metals, alkaline earths), oxide glasses

The authors would like to acknowledge support from the National Science Foundation through CIAN NSF ERC under grant #EEC-0812072.

based on non-silicate systems are also of interest, primarily in the area of specialty fibers providing unique emissive (through lanthanide ion dopant addition) or nonlinear optical properties. Examples of such systems include tellurite glasses (TeO_2-based) and phosphate (P_2O_5-based) glasses.

***Fluorides*:** Originally discovered in 1975 at the Universite de Rennes, these glasses are based on a network structure involving fluorine as the anionic constituent. Primary interest in this system is focused on those compositions containing heavy-metal components (e.g. Zr) together with lighter metals added to improve material resistance to devitrification and to improve chemical durability (i.e. resistance to water and oxygen attack). One of the most stable fluoride glass compositions used for fiber development is based on a mixture of fluorides of Zr, Ba, La, Al, and Na (ZBLAN). Fluoride glasses typically exhibit reduced resistance to devitrification compared with silicates and are also prone to degradation under moist environmental conditions. Moreover, the glass forming composition ranges are limited compared to silicates. Thus, while the optical properties of these materials offer increased opportunity for specialized applications based on their infra-red transmission, fiberization requires increased care and often unique preform development and fiber draw methodologies to address the chemical, thermal, and phase stability of these materials.

***Chalcogenides*:** These glasses are based on chalcogenide anionic constituents (i.e. containing S, Se, and Te). Additional metal and non-metal elements (e.g. Cd, As, Br, P, I, etc.) are added for property control. Again, of great interest for long wavelength transmission applications, it is worthwhile to note that some families of chalcogenides are known to exhibit unique optically induced structural and property changes that can have significant technological benefit for patterned or tailored material functions.

Organic (Plastic) Optical Fibers (POF)

The need for inexpensive, mechanically robust fiber optic options for digital data transfer over short transmission lengths has spurred the development of organic polymer optical fibers. Such fibers offer enhanced strength and mechanical flexibility, lower temperature forming processes, increased economy in material costs, and the ability to be readily connected and spliced using injection-molded components.

Polymeric fibers, however, typically exhibit much greater attenuation throughout their primary optical transmission window (i.e. visible) than that of their silica fiber counterparts. This is due to the organic structural units (e.g. C-H bonds) participating in the polymer structure that exhibit fundamental and overtone absorption resonances that produce absorption bands in the visible and significantly limit the long wavelength (red) transmission of the material.

Polymethylmethacrylate (PMMA) is commonly used as the polymer core material for plastic optical fiber structures. In an effort to reduce absorption losses, hydrogens in some polymer structures are replaced with fluorine (a heavier atom). These fluorinated materials include CYTOP, a fluorinated polymer made by Asahi Glass.

The authors would like to acknowledge support from the National Science Foundation through CIAN NSF ERC under grant #EEC-0812072.

2.5 Optical Fiber Geometry

In addition to the bulk material optical constants (n, κ) and their wavelength dispersion, the physical geometry and index profile of the optical fiber cross-section, determines the spatial confinement and modal propagation characteristics for light within the fiber structure. While greater detail concerning the physics of light guiding will be provided in later Modules, the fiber structure design that evolves from this discussion represents the fundamental target for the fabrication process. In this context, a brief overview of key fiber design types and characteristics will be offered here to provide a background for subsequent discussion of preform development and fiberization techniques.

Light Refraction

Optical fibers, like any optical waveguiding structure, effectively confine light to propagate within a dielectric material structure by controlling the material refractive index profile (i.e. defining the core and cladding regions) across the waveguide cross-section. In contrast to planar waveguides (dielectric slab waveguides), optical fiber light guiding, and its analysis, is based on a cylindrical geometry. Insight into the general characteristics of a refractive index distribution consistent with light guiding can be obtained by examination of Snell's law to describe the refraction of light at an interface between two materials:

$$n_1 \sin\varphi_1 = n_2 \sin\varphi_2 \qquad \textit{(Equation 2.12)}$$

where the subscripts are defined in **Figure 2.8**.

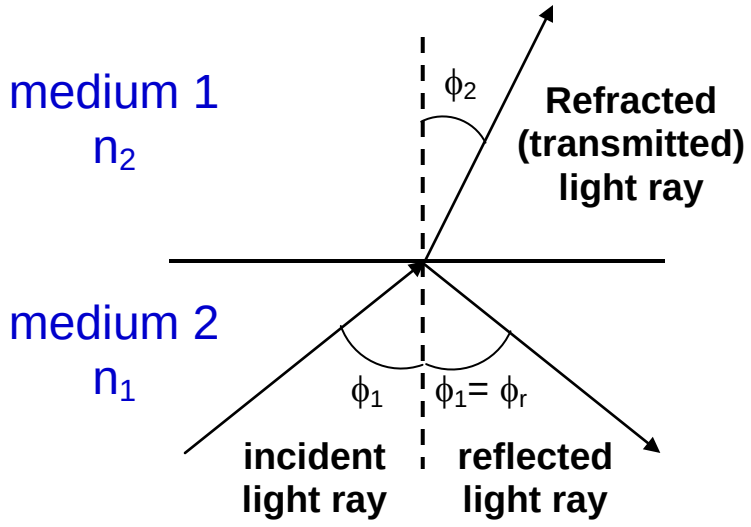

The authors would like to acknowledge support from the National Science Foundation through CIAN NSF ERC under grant #EEC-0812072.

Figure 2.8: *Reflection and refraction at an interface between two media. The refracted angle is given by Snell's law.*

In the Figure, for light incident on the interface from medium 1 with an incidence angle of phi1, Snell's law allows the angle of refraction, phi2 to be determined within medium 2. Clearly, as the incidence angle is increased, the refraction angle will also increase. If n1>n2, an incidence angle can be selected to produce an angle of refraction = 90 degrees, corresponding to light propagation along the interface between the two materials. Beyond this "critical" angle, light will be reflected at the interface. Note that this condition for "total internal reflection" can only be met when light is propagating from a medium of higher refractive index to a medium of lower refractive index. Thus, in the context of an optical fiber, light will remain confined within the core of the fiber when its angle of incidence to the core-clad interface is greater than the critical angle for total internal reflection. At this point, light injected into the fiber core can be thought to bounce back and forth between the core-clad interface as the light propagates down the length of the fiber. This will only occur if the index of the core material is larger than that of cladding material.

To illustrate the conditions for total internal reflection light propagation is simplified by ray-tracking. A more complete analysis of optical propagation characteristics involves the development of guided-wave modes based on electromagnetic wave theory, and associated boundary conditions, within dielectric layers of various geometries. Through this approach, it can be shown that only a discrete set of modes exist that will propagate along a given fiber geometry and index profile. From a ray-tracing perspective, for example, this quantization of propagating mode characteristics corresponds to a set number of incidences angles (still greater than the critical angle) that will result in light guiding. Modal analysis is the key to understanding of a variety of fiber performance characteristics, providing information on the electromagnetic field distribution for specific propagation modes in relation to the index profile and furnishing the framework for fiber geometry and index profile design and optimization for a specific application. The interested reader is referred to Module 3 (Wave Propagation) and references therein for a more complete discussion.

Fiber Types

As discussed previously, optical fibers consist of an inner core region and an outer cladding region. The inner core material is fabricated so that it has a higher refractive index than the cladding material. A buffer or jacket layer is commonly coated over the cladding layer in order to provide additional mechanical strength and to provide protection from water or other environmental contaminants.

In terms of light guiding performance, optical fibers are typically categorized as either single or multimode fibers depending upon the number of guided wave modes that can be supported by the fiber structure. As mentioned above, the geometry of the core-clad structure and the index profile determine whether the fiber can support guiding in more than one mode. In general,

The authors would like to acknowledge support from the National Science Foundation through CIAN NSF ERC under grant #EEC-0812072.

larger diameter cores and greater refractive index differences between the core and the clad material favor the support of multiple guiding modes at a given wavelength within the fiber. The two primary core/clad refractive-index profile types are shown below.

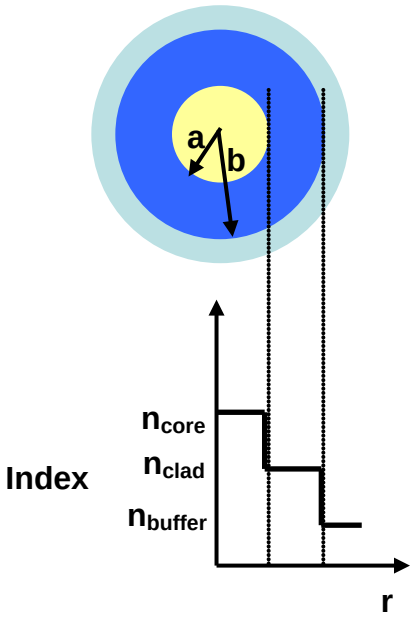

Figure 2.9: *Step-index fiber geometry.*

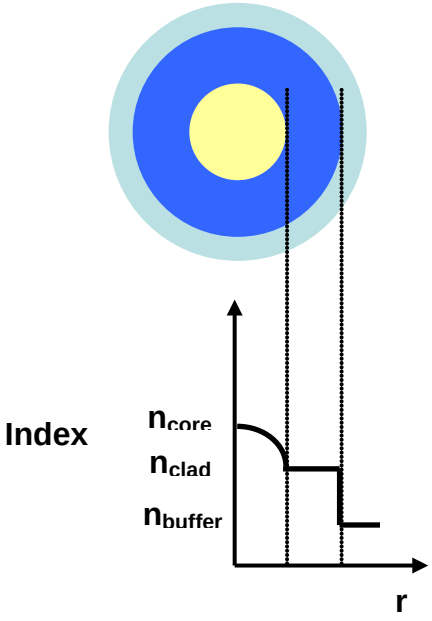

The authors would like to acknowledge support from the National Science Foundation through CIAN NSF ERC under grant #EEC-0812072.

Figure 2.10: *Gradient-index fiber geometry.*

For a fiber with a core radius (a) and a cladding thickness (b-a), two types of refractive index profiles are shown in **Figure 2.9** and **Figure 2.10**. The first fiber geometry is known as a step-index fiber profile. In this case, the refractive index of the core is uniform throughout and undergoes an abrupt change (step) at the cladding interface. The second common fiber geometry is the gradient-index profile. This fiber type is characterized by a continuously varying refractive index in the core region that, typically, decreases as the core radius increases until it reaches the refractive-index value of the cladding at the cladding interface. Manipulation of the core index profile provides additional opportunity to tailor the light propagation characteristics (e.g field profiles, effective indices, modal dispersion).

Conditions for light guiding within core-clad fiber structure

Returning again to a description of guided wave propagation in terms of ray-tracing of internally reflected light, **Figure 2.11** depicts ray propagation within a core-clad structure. The Figure helps to illustrate the light injection conditions necessary to excite a propagating mode within the structure. Through Snell's law, the minimum angle that will satisfy conditions for total internal reflection at the core-clad boundary is given by:

$$\sin\phi_{\min} = \frac{n_2}{n_1} \qquad \textit{(Equation 2.13)}$$

In the diagram below, ray C represents the critical angle and total internal reflection.

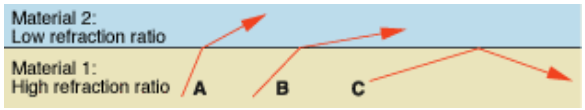

Figure 2.11

Again referring to **Figure 2.11**, the condition for total internal reflection, defined by the internal fiber structure and index step, will dictate the maximum entrance angle, $\phi_{\max}$ for light entering through the air-fiber interface:

$$n\sin\phi_{0,\max} = n_1\sin\phi_c = (n_1^2 - n_2^2)^{1/2} = NA \qquad \textit{(Equation 2.14)}$$

where the variables are defined as in **Figure 2.11**.

The above equation also serves to define a useful parameter of the step-index fiber called the numerical aperature (NA). Since it is directly related to the maximum angle of acceptance to provide guiding in the fiber, the NA is typically used to describe a fiber's light gathering

The authors would like to acknowledge support from the National Science Foundation through CIAN NSF ERC under grant #EEC-0812072.

capability. Values of NA typically range from 0.14 to 0.5 and are always less than one (for insertion of light from air).

Modal analysis can not be derived by ray-tracing models, yet is an important consideration in fiber design. This analysis involves the solution of Maxwell's equations under appropriate boundary conditions as described in Module 3. Such an approach reveals that the allowable propagation characteristics are quantized, allowing only specific "modes" to propagate along the core-clad structure of the fiber. Each mode is defined by a specific EM-field profile and effective propagation characteristics. (In the context of ray-tracing, the modal analysis essentially indicates that only specific incidence angles (above the condition above the critical angle for total internal reflection) will excite a guiding mode.)

From the modal analysis, minimum requirements to support a guiding mode within the fiber structure are defined in terms a "cut-off" condition for the propagation wavevector for a mode, below which light will not be guided within the core. The cutoff condition is directly related to the cladding index (n_2) the wavevector ($k = 2\pi/\lambda$) for the incident light. The "V-parameter" is closely related to this cutoff condition and can be used to determine how many modes may be supported by a given fiber geometry and refractive index profile.

$$V = \left(\frac{2\pi a}{\lambda}\right)(n_1^2 - n_2^2)^{1/2} = \frac{2\pi a}{\lambda} NA \qquad \textit{(Equation 2.15)}$$

where: a = the core radius; λ = incident light wavelength.

For a multimode fiber, the V parameter is large and the number of guided modes, M, possible can be estimated by:

$$M \approx \frac{1}{2}\left(\frac{2\pi a}{\lambda}\right)^2 (n_1^2 - n_2^2) = \frac{V^2}{2} \qquad \textit{(Equation 2.16)}$$

Thus, as mentioned above, the number of guiding modes supported by a given fiber design is dependent upon the core-clad index difference, the fiber geometry, and the wavelength of the propagating light. Note that these metrics are developed for step-index fibers. Analogous parameters relationships can also be developed for graded refractive index profiles.

2.6 Perform Fabrication Techniques

Optical fiber preform fabrication can be accomplished using vapor-phase deposition or condensed phase assembly techniques to produce the required core-clad index geometry. While early production of silicate glass fibers from preforms was pursued using condensed phase assembly methods (e.g. rod-in-tube), the demand for low-loss fibers for telecommunication drove the development of vapor-phase methods that allowed the use of high-purity components and improved material synthesis techniques. The following discussion is not intended to furnish

The authors would like to acknowledge support from the National Science Foundation through CIAN NSF ERC under grant #EEC-0812072.

an exhaustive list of techniques and issues in preform fabrication but, rather, to focus on a few common and relevant fabrication techniques.

Vapor-phase deposition techniques for the production of silica-based optical fiber preforms involve the high-temperature oxidation of metal-chloride (or, more generally, metal-halide) precursor vapors (e.g. $SiCl_4$, $GeCl_4$, other dopant-metal chlorides) to produce the amorphous particulates of required oxide material. The reactant vapor constituents and stoichiometry determine the composition of the resulting material. The approach typically results in a porous "soot" of the oxide particles that is then sintered into the final glassy preform material. Variants of this vapor deposition approach are differentiated by the specifics of the deposition geometry and reaction conditions used.

Outside Vapor Deposition (OVD)

Figure 2.12 contains a schematic of the general OVD process. In this method, the precursor chlorides are flame hydrolyzed within a methane/oxygen torch to form the oxide soot material and deposited laterally onto a rotating rod or mandrel. The cylindrical rod is repeatedly passed through the soot flux from the burner while being rotated to allow the uniform, multilayer deposition of material along the rod length. Variation in precursor composition with time can be used to alter the radial composition of the soot material, thus influencing the final refractive index profile of the final preform. The technique thus can be used to produce both step and gradient index fiber designs. The mandrel is often either graphite or a ceramic material which is removed upon completion of the deposition process. The resulting porous tube of deposited material is then sintered (T = 1300 °C – 1500 °C for silica-based systems) and vitrified under high temperatures to produce a hollow glass preform with the intended index profile for the fiber. Prior to the final sintering step, the soot material is dried by heating to high temperatures (near 1000 °C) under a chlorine atmosphere to remove hydroxyl species left from incomplete oxidation of the precursors during deposition. The central hole in the preform collapses during the final fiber drawing process. **Figure 2.13** depicts heating the preform to collapse it and then draw from it the final optical fiber.

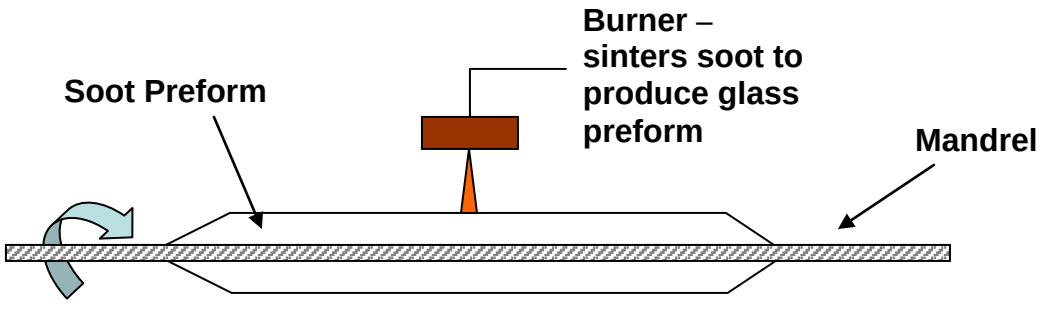

Figure 2.12: *Outside Vapor Depsition technique.*

The authors would like to acknowledge support from the National Science Foundation through CIAN NSF ERC under grant #EEC-0812072.

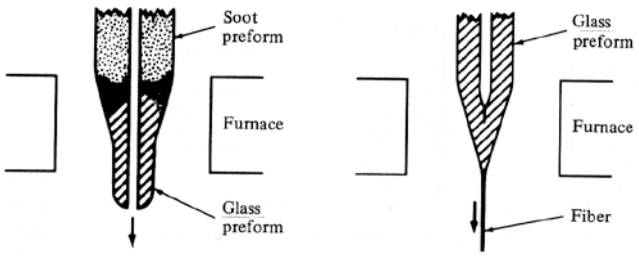

Figure 2.13: *Preform rod heating and collapse followed by final fiber draw to produce optical fiber.*

Vertical Axial Deposition (VAD)

The VAD method contrasts the OVD process in that the core and clad soot materials can be deposited using two different burners simultaneously (see **Figure 2.14**). The core material is deposited end-on to a seed rod while the clad material is deposited laterally. The rod is drawn up vertically as deposition proceeds. In this way, a solid preform cylinder (no central hole) is developed. In further contrast to the OVD method, the composition/index profile in the VAD approach is derived from control of the precursor stoichiometry in the respective torches used but also through control of the temperature profile generated across the soot surface. As with the OVD process, the porous soot cylinder is sintered under similar conditions after deposition is complete.

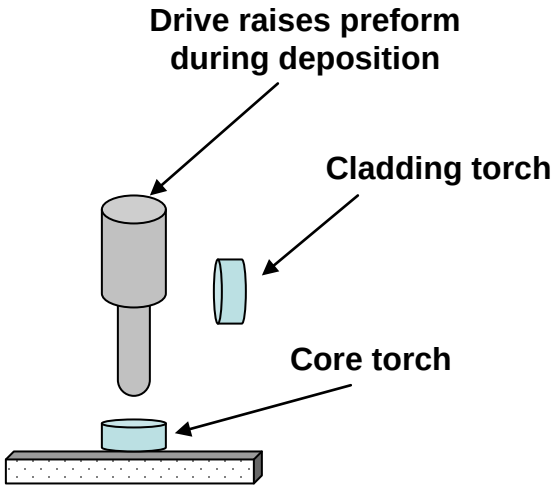

Figure 2.14: *VAD preform fabrication technique.*

The authors would like to acknowledge support from the National Science Foundation through CIAN NSF ERC under grant #EEC-0812072.

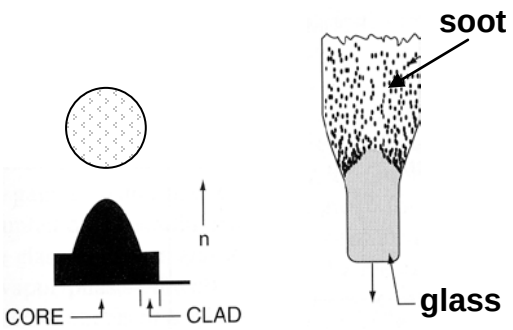

Figure 2.15: *VAD preform index profile (left) and sintered preform rod (right).*

Modified Chemical Vapor Deposition (MCVD)

The MCVD method involves the reaction and deposition of fiber materials within a silica substrate (bait) tube. Chloride-based precursors are reacted with oxygen within a hot-zone generated by a movable oxy-hydrogen torch external to the reaction tube. The resulting gas phase reaction forms submicron particles that form a deposit downstream of the hot-zone on the inside wall of the silica tube.

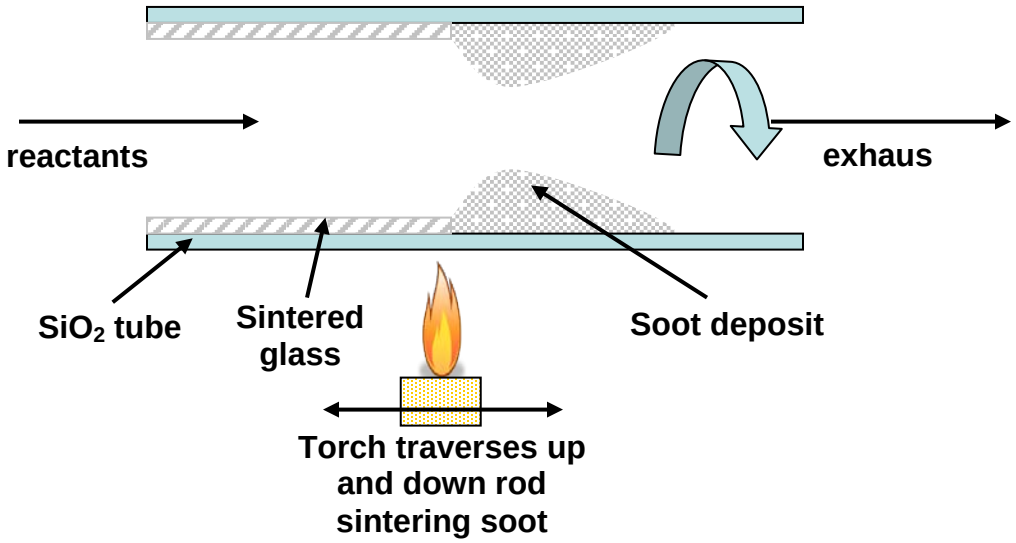

The authors would like to acknowledge support from the National Science Foundation through CIAN NSF ERC under grant #EEC-0812072.

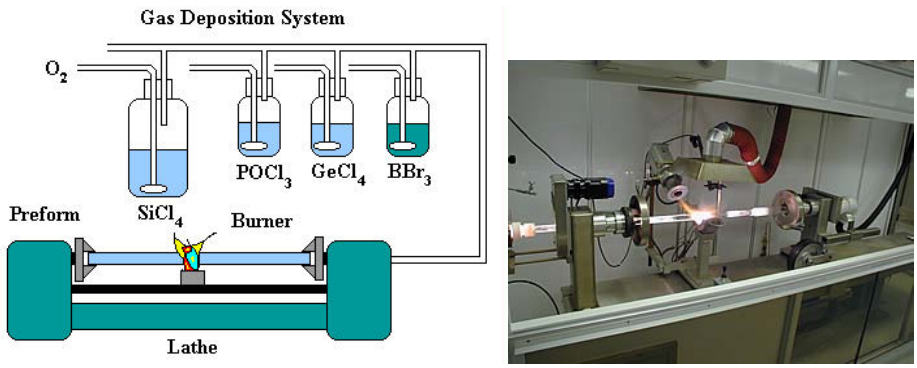

Figure 2.16: *MCVD deposition apparatus.*

Figure 2.16 shows a general schematic of an MCVD apparatus and a photograph of a working system. The soot is sintered in-situ as the oxy-hydrogen torch passes along the length of the deposit and the tube is simultaneously rotated on a glass working lathe to insure uniform processing around the circumference of the developing preform. As with the OVD process, the core and clad glass compositions (and resulting index profile) are obtained by control of precursor gas composition with time as the multilayer deposition proceeds. Typically up to 100 layers of material are produced, depending upon whether the fiber to be produced is single or multimode. Once the desired glass thickness is obtained using the iterative, soot-deposition/sintering process, the reactant gas flow is terminated and the tube is heating sufficiently to cause it to collapse, forming a solid preform rod. The original silica reaction tube thus serves as the clad material and the deposited glass provides the core.

Plasma Chemical Vapor Deposition (PCVD)

Similar to MCVD, in that a precursor gas stream is reacted within a substrate tube, the PCVD technique utilizes a low-pressure (approx. 10 Torr), non-isothermal microwave plasma to initiate the oxidation reaction and the deposition of glassy material from the vapor. Vapor diffuses to the tube walls (typically held at near 1100 C to minimize mechanical stresses in the evolving film) and heterogeneously reacts to form a deposit, thus avoiding the formation of a soot and the associated sintering step. In a similar manner to the torch used in the MCVD technique, the microwave generator traverses the length of a rotating reaction tube during material deposition. While the microwave process is rapid, enabling the efficient production of multimode preforms, the deposited material typically retains higher hydroxyl concentrations and the potential for increased optical losses in the final fiber. Fluorine dopants (e.g. C_2F_6) are often added to the reaction stream to address this issue.

Overcladding

The authors would like to acknowledge support from the National Science Foundation through CIAN NSF ERC under grant #EEC-0812072.

While the core and primary clad structure of the optical fiber can be produced using the above techniques, an overcladding layer is typically added to the outside of the preform rod to increase the overall preform mass and increase the length of fiber that can be drawn from a single preform. In this case, the overcladding can be produced by inserting the original preform into a second silica tube to increase the outer diameter of the preform or by using the initial preform as a "bait" rod for OVD or VAD deposition of additional clad material. [see, for example, MacChesney]. Preforms to be used with overcladding frequently have oversized core regions to obtain the targeted core/clad radius ratio in the final, overcladded, preform.

Condensed Phase Methods

Precursor chemistry and physical properties coupled with difficulties in the production of suitable reaction conditions can limit the use of the vapor phase deposition techniques for the formation of fiber performs based on non-silica (and/or non-oxide) glass systems. In this case, alternative approaches, involving the physical or melt-based assembly of core and clad glass preform elements, are utilized. Some of these techniques are employed for silicate glass preform fabrication for specialty applications and were also used for preform development prior to the development of the vapor phase methods described above. Other techniques make use of unique thermo-rheological properties available in some alternative glass forming systems.

Rod-in-tube

A relative easy, low-cost method, the rod-in-tube approach involves the production of a core glass rod and cladding glass tube via conventional melting and forming procedures. Oxide and non-oxide (e.g. fluoride-based) glasses often make use of this technique. The overcladding technique described earlier is a variant of this approach in which the vapor-phase deposited preform is substituted for a homogeneous core glass rod.

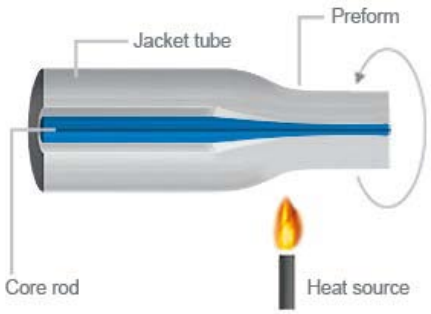

Figure 2.17

The core rod is inserted into the tube and the assembly is drawn directly into a fiber. Both the rod exterior and the cladding tube interior surfaces are thoroughly cleaned and polished prior to insertion of the rod to minimize the development of inclusions or gas bubbles (producing

The authors would like to acknowledge support from the National Science Foundation through CIAN NSF ERC under grant #EEC-0812072.

additional optical losses as light propagates down the fiber core) at the core-clad interface. The rod and tube are then fused together under high temperature to form a monolithic preform. High numerical aperture, step-index performs can be easily produced in this manner. The requirements for physical manipulation of narrow rod geometries and small bore tubes during preform assembly typically limit this approach to the development of multimode fibers. Core-clad interfacial losses also typically limit the use of rod-in-tube fabrication to specialty fiber applications, including fiber lasers where the core material contains an optically emissive rare-earth dopant.

A number of techniques were developed to address preform fabrication challenges inherent in fluoride glasses [see Aggarwal]. These involve the formation of preform geometries via a combination of glass casting and physical assembly steps. The mold material used for casting limits the suitability of these approaches for glasses exhibiting compatible melting temperatures. In low melting point fluorides, for example, the mold material is typically brass.

Build-in casting

This technique involves the casting of the clad glass composition into a preheated (near Tg) cylindrical mold. Immediately upon filling, the outer surface of the glass (in contact with the mold) begins to cool and solidify. Before complete solidification, the mold is inverted and the still-molten glass near the center allowed to flow out, leaving a hollow cylinder (the clad) behind. The core glass composition is then poured into the clad cylinder and allowed to completely cool and solidify. **Figure 2.18** depicts a schematic of the build-in casting process. After core casting, the preform is then annealed to remove residual stresses arising from differences in cooling rate and from the variation in thermal expansion coefficient due to the different glass compositions of the clad and core. The finished preform is then removed from the mold.

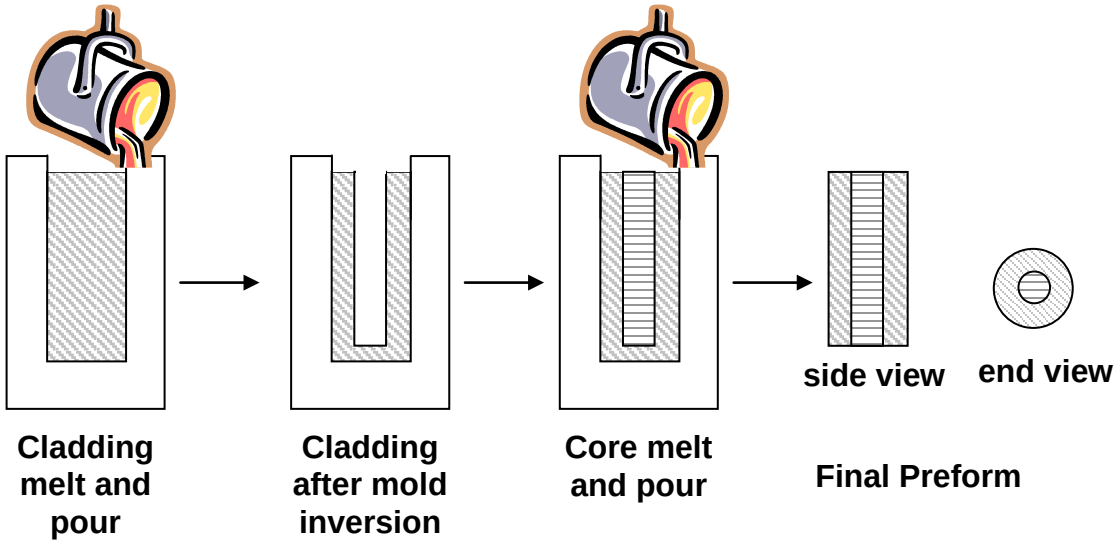

The authors would like to acknowledge support from the National Science Foundation through CIAN NSF ERC under grant #EEC-0812072.

Figure 2.18: *Schematic of the build-in casting technique*

The approach typically produces a higher quality core-clad interface (and reduced scattering losses) because the interface is formed while the glasses are in liquid form. One drawback, however, involves a continuously varying core-to-clad ratio along the preform length.

Rotational casting

The tapered core-clad geometry of the build-in process is addressed in this technique through the rotational casting process. In this case, a limited amount of cladding glass is added to a cylindrical mold (again preheated to near Tg). The mold is integrated into a lathe apparatus, allowing it to be immediately rotated rapidly (1000's of rpm) while in a horizontal orientation within a concentric tube furnace, thus forming a hollow cladding tube. The amount of glass added in the initial step controls the final inner diameter of the uniform cylindrical tube formed. Core glass material can then be cast directly into the cladding tube followed by annealing.

Modified build-in casting

In this approach, cladding glass again fills a cylindrical brass mold. However, before the center glass volume solidifies, a volume of core glass is poured on to the top of the clad and a bottom plate of the mold is removed, allowing the unsolidified clad glass and the entrained core glass to be drained. The process thus creates the core-clad structure directly from the two melts in a single solidification step. Careful control of glass and mold temperatures, timing of the core glass pour, and glass thermal properties is critical to insure a uniform core-clad ratio along the preform length at the desired value.

Suction casting

Developed for the production of single-mode fluoride fiber performs, this technique again involves the filling of a cylindrical mold with cladding glass followed by core glass. In this case, the mold incorporates a reservoir at the bottom whose size can be used to control the total amount of glass volume change upon cooling. As the clad-core melt solidifies, the clad glass contracts within the reservoir and the still-fluid clad glass along the center axis of the mold moves downward, producing a suction force that pulls the core glass down along the center of the preform. The strategy requires close control of reservoir volume and mold diameter to insure accurate control of core-clad radius ratio and preform length.

2.7 Double-crucible technique

The preform-based drawing approach is inherently a batch-type process, given the finite length of the preform itself. Early efforts at lower melting temperature silicate glass fibers resulted in the development of a double crucible method in which core and cladding glasses are placed in separate, concentric crucible containers (typically platinum) with a common orifice at the bottom. Feed materials can be continuously supplied at the top of the crucible thus producing a

The authors would like to acknowledge support from the National Science Foundation through CIAN NSF ERC under grant #EEC-0812072.

technique for continuous fiber fabrication. The crucible is held within a furnace under a controlled, inert gas atmosphere. At the appropriate temperature, a stream of core glass passes through the clad glass as it exits the crucible, forming the core-clad structure. In addition to step-index fibers, interdiffusion between the core and clad while in contact within the crucible orifice enables the development of an index gradient as well. Moreover, the core-clad interface is formed directly from the melt, advantageous for lower scattering losses. However, significant problems with contamination and the resulting impurity optical absorption, as well as the inability to closely control refractive index profile in the finished fiber, reduced the utility of this technique, particularly in light of developments in preform production (see above). Moreover, the technique is not applicable at the temperatures required for high silica fiber optic fabrication. While not a primary method for telecommunications fiber manufacture, the technique is still used for the development of some non-oxide (low melting temperature) glass fibers (e.g. chalcogenides) for specialty applications.

2.8 Optical Fiber Drawing

Drawing from a preform

Preform-based fiber drawing involves the localized heating of the preform above the glass softening point to allow the glass to elongate and reduce its diameter ("neck-down") into the smaller diameter filament needed. The drawing process produces a reduced scale replica of the preform cross-section, hence the importance of accurate preform design and fabrication. A uniform drawing stress is applied to the end of the filament to continue the elongation process as additional preform material is fed into the hot zone of the drawing furnace. A typical overall fiber diameter for telecommunications applications is 125 microns defining a draw-down ratio from the preform diameter from 10:1 to 100:1 depending upon the specific preform used. Control of fiber diameter uniformity is critical to low-loss operation and insured compatibility with cabling and splicing needs. Moreover, fiber strength must be maintained to allow handling without breakage. As discussed in Module 1, high fiber strength is intimately dependent on maintaining a pristine surface, free from flaws. Hence, the as-drawn fiber does not contact a solid surface until it receives a protective polymer coating, applied in-line.

The total apparatus used to produce optical fibers is called a "drawing tower" and contains functional components responsible for maintaining the necessary thermal, mechanical and environmental conditions needed for high reliability fiber production. **Figure 2.19** contains a photograph of an actual draw tower (the take-up drum is on the right-hand side of the picture). A typical fiber draw tower schematic is provided in **Figure 2.20**. Control of contamination requires that low-loss fiber manufacturing be pursued under clean-room conditions.

The authors would like to acknowledge support from the National Science Foundation through CIAN NSF ERC under grant #EEC-0812072.

Figure 2.19: *Fiber draw tower (from optics.org/cws/article/research/25393/1/drawtower)*

The authors would like to acknowledge support from the National Science Foundation through CIAN NSF ERC under grant #EEC-0812072.

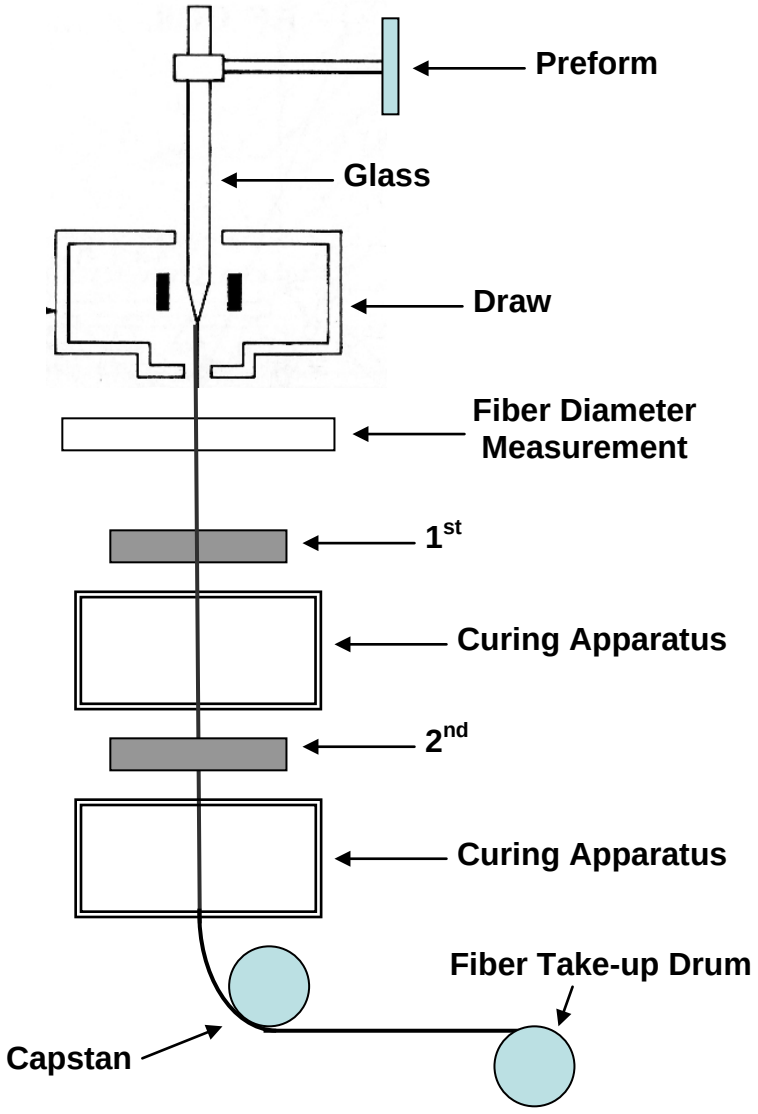

Figure 2.20: *Schematic of fiber draw tower.*

Four basic components of the fiber drawing process are represented in the **Figure 2.20**: a) a heat source, b) the glass feed system, c) stress application to draw the fiber, and d) a support structure that aligns these elements. In addition, the draw tower also contains process monitoring and feedback equipment to maintain an efficient, continuous draw process over the lifetime of the preform and in-line coating/curing systems to apply protective coatings prior to contact with the tensioning elements (capstan) and winding ("take-up") drum or spool. Different functional components or processes of fiber drawing are discussed below:

Heat source

The authors would like to acknowledge support from the National Science Foundation through CIAN NSF ERC under grant #EEC-0812072.

Heating of the end (or "root") of the fiber preform to above its softening point is fundamental to the drawing process. As noted in previous discussion, long-haul, low-loss telecommunications grade fiber is silica-based, requiring preform heating to between 1900 and 2200 °C. This temperature profile must be produced at a localized point at the preform end and must be uniform around the entire preform circumference and concentric to the fiber axis to insure a circular cross-section fiber. Several heating technologies have been pursued to satisfy these rather stringent requirements, including H_2-O_2 burners, CO_2 laser heating, electric (resistive) furnaces, and zirconia induction furnaces. Most common are graphite resistive furnaces and the zirconia induction furnace. The former, however, requires an inert atmosphere to operate as the resistive element will oxidize under air conditions at these temperatures. The need for controlled atmosphere is avoided through the use of the induction furnace in which the zirconia tube defining the heating region also serves as the heating element. This approach also reduces contamination from heating elements commonly observed in resistive heated systems.

Preform feed and draw speed

As the preform is fed into the furnace conservation of mass dictates that the rate at which glass volume enters the furnace (as a preform) must equal the rate at which it emerges (as a fiber) under steady-state drawing conditions. This can be represented in an analytical expression that embodies key process parameters of fiber drawing, i.e. the preform feed rate (S) and the fiber draw speed (s):

$$s = S\left(D^2 / d^2\right) \qquad \textit{(Equation 2.17)}$$

where: D = preform diameter, d = fiber diameter.

Typically, the fiber draw speed is used as the primary adjustable parameter to maintain a given fiber diameter, with the preform feed rate and furnace temperature maintained at a constant values. Referring to the previous equation, variations in fiber diameters of no more than 1% require a total variation in preform feed rate and draw speeds of less than 2%. Common draw speeds in telecommunications fiber manufacture are typically in the tens of meters/sec range.

A common approach to achieve control in draw speed involves the use of a low inertia tractor device (e.g. capstan) (see **Figure 2.20**) that is driven by a motor capable of rapid (high bandwidth) speed changes in response to diameter measurement information. Fiber passes over the capstan for spooling under a controlled winding tension that can be less than the drawing tension using this method. In another variant, fiber draw tensioning can also be supplied directly by a high-inertia drawing component (e.g. winding drum) that helps to maintain the draw speed

The authors would like to acknowledge support from the National Science Foundation through CIAN NSF ERC under grant #EEC-0812072.

under the influence of high frequency perturbations. However, the large mass also makes fine adjustment of the system more difficult.

Diameter measurement and control

While the above equation provides a means to relate process conditions (draw speed, preform feed rate) to the resulting fiber diameter, maintaining a precise diameter (typically fiber diameter must be maintained to within 1 micron of the target) requires rapid, accurate measurement of fiber diameter in real-time as it exits the draw furnace and a responsive feedback loop to draw tower elements capable of influencing the fiber draw/preform feed rate ratio. As mentioned above, typically the in-situ fiber diameter information is used to adjust fiber draw rate. This is accomplished by adjusting the rotation speed of the take-up drum (see **Figure 2.20**) . Practically speaking, the development of a complete control system is needed, requiring that time lags between diameter error formation, measurement, draw condition adjustment, and draw system response be accurately characterized. Control theory is often used to examine these response times for each of the key elements in the loop and provide models useful in establishing a stable feedback situation.

In-situ, rapid non-contact diameter measurement on the draw tower is needed to provide the metric used to adjust draw conditions. The measurement is usually performed close to the furnace exit for the fiber to minimize delay in determining the diameter for the process control. Diameter measurement methods are based on generally two primary optical phenomena: shadowing (light blocking) and light scattering. Light scattering can be observed in forward- and backscattering modes with the fiber diameter computed by the examination of interference fringe patterns generated after incident, collimated laser light interacts with the glass fiber. Many variants on optical measurement strategies exist, differentiated by geometry, optical phenomena of interest, and analysis approach.

A very important aspect of the draw conditions that contribute to consistent diameter control is the local atmosphere and mechanical stability in the region of the furnace and, more precisely, along the length where the preform is elongated to achieve the fiber diameter (i.e. the “neck-down” region). The fiber in this range is still fluid and its geometry can be easily disturbed. Given the vertical orientation of the furnace, convective air currents, and the introduction of purge gases to protect resistive heating elements, turbulence can result in rapid, local changes in fiber diameter. Seals, irises, and close clearances at the preform entry and fiber exit points in the furnace must be used to minimize these effects. Similarly, the tower assembly must be rigid and mechanically isolated from its surroundings to avoid vibration transmission to the fiber during drawing.

Coating application

Providing primary protection from mechanical abrasion and the minimization of microbending during subsequent handling, polmeric coatings are applied in-line onto the fibers after they exit the draw tower furnace and diameter-measurement stage. Primary design criteria for coatings

The authors would like to acknowledge support from the National Science Foundation through CIAN NSF ERC under grant #EEC-0812072.

include: dimension (thickness), mechanical characteristics, and chemical characteristics and stability. In general, the coatings provide an intermediate encasement of the optically active fiber structure for subsequent incorporation into cabling. The competing requirements for increased cable capacity (more fibers/cable) and the mechanical protection of the fiber itself are often a focus of design compromise in terms of coating thickness, for example.

Coating mechanical behavior, including toughness, strength, elastic and viscoelastic properties, also contribute to the design of coating systems. In addition to the long-term environmental chemical stability of the coating, coating materials must readily wet and bond to the fresh glass surface to provide good adhesion. Thus, knowledge of silica surface chemistry and its interaction with organic coating systems is of key interest in the development of surface treatments for coating application. It is also interesting to note that coating chemistries also must typically provide a means for its removal to allow splicing and connectorization operations. Both mechanical and chemical stripping methods are employed.

Polymer coating materials can be applied to the fiber either from a melt or by application and subsequent UV-induced polymerization (curing) of the appropriate monomer or oligomer. One approach for the latter is the use of a pressureless die (open cup applicator). Here, the fiber passes through a reservoir filled with coating fluid and exits through a die at the bottom that determines the geometry of the coating on the fiber and, hence, the final coating thickness. Typically a guide is included in the reservoir to help direct the fiber through the tapered die. For monomer or oligomer coatings, the fiber is then typically passed through a UV-cure step.

Pressurized dies, where the coating material is injected onto the fiber surface, have also been developed to facilitate greater control of the coating fluid application conditions and the ability to move to faster drawing speeds. A variety of coating chemistries (usually based on acrylate chemistry) can be used, often incorporating photoinitiators (for UV-curing) and additives to promote adhesion and to manipulate coating viscosity and curing speed. Often a dual coating system is utilized employing primary and secondary coating and curing processes on the fiber draw tower. In this case, the primary coating (nearer the optical fiber clad material) is a high elastic modulus, hard, high Tg material providing primary protection against mechanical damage and bending stresses. The secondary coating allows for labeling of the fiber (good ink adhesion) and improves mechanical behavior for fiber handling and storage (e.g. winding, cable integration).

(low melting temperature) glass fibers (e.g. chalcogenides) for specialty applications.

2.9 Cabling

Given the inherently brittle nature of optical fibers and their susceptibility to weakening through mechanical handling, exposure to moisture, and static or cyclic stress, practical application of fibers in the field requires their integration into a cable structure. Designed for specific applications and installation environment requirements (e.g. interior, exterior, underground, submerged, suspended, etc.), cables allow the optical fibers to be used while providing the

The authors would like to acknowledge support from the National Science Foundation through CIAN NSF ERC under grant #EEC-0812072.

mechanical and chemical protection necessary for reliable optical transmission. In addition to maintaining fiber optical performance, cable designs must also address issues of importance to cable manufacturability, practical use, and installation and maintenance, including: ease of splicing and handling, volume (space efficiency) and weight.

As an example, **Module 1** discussed the impact of surface flaws on the statistics of brittle failure in glass. In that context, the longer the glass fiber, the more likely a critical size flaw exists that will promote failure under sufficient stress. The desire to produce long cabling lengths (and minimize connections between lengths) thus implies that these fibers must be fabricated and successfully integrated into the cable design while avoiding such flaws. Recognizing that cable lengths are intended to be kilometers long, this requirement is a primary challenge.

The brittle nature of the glass fibers also implies a limited available strain (or elongation in tension) available before failure. Reasonably good fiber breaking strains fall within 0.5 to 1%. This is compared with copper used in conventional electrical cabling in which plastic strain can be as high as 20% before failure. In this case, the copper itself is often the primary load bearing element in an electrical cable whereas another load bearing element (metal wire, plastics, organic yarns (Kevlar)) must be integrated into the optical fiber cable to avoid the transfer of tensile stress to the fiber during installation and use. Additional design approaches to minimize mechanical impact and stress application to the fiber include: isolation of other cable components from the fiber, positioning of the fiber near the neutral axis of the cable, and providing free volume near the fiber to allow it to move to positions of reduced stress when the cable is bent or stretched. These design goals can be achieved by routing the fiber (coated with a buffer or jacketing material for added protection) within a semi-rigid polymer tube (e.g. polyethylene) whose inner diameter is larger than that of the coated and jacketed fiber.

As mentioned above, cable designs are many and varied, depending upon the use conditions and the specific applications. Single and multifiber cable designs are both common. An example of both a single fiber cable and of a five-fiber cable design is provided in **Figure 2.21** illustrating the general construction and use of materials to address the functional requirements discussed above. Depending upon the number of fibers to be incorporated into the cable, overall geometries vary from the circularly symmetric cross-sections depicted in the figures (for smaller numbers of fibers) to more planar or ribbon-like arrangements for high-bandwidth cabling that promote easier handling and the opportunity for simultaneous splicing of multiple fibers.

The authors would like to acknowledge support from the National Science Foundation through CIAN NSF ERC under grant #EEC-0812072.

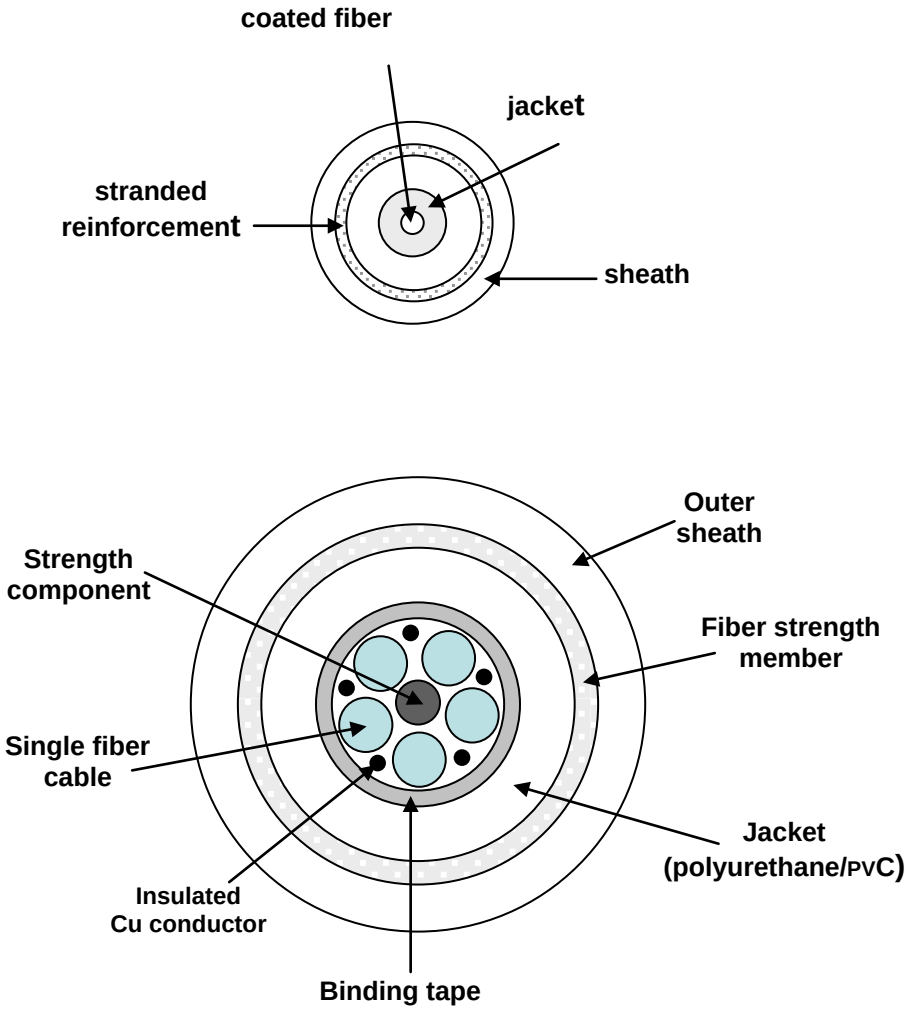

Figure 2.21: *A single-fiber cable design (top) and a multi-fiber cable design (bottom).*

The authors would like to acknowledge support from the National Science Foundation through CIAN NSF ERC under grant #EEC-0812072.